

Assessment of environmental effects in scour monitoring of a cable-stayed bridge simply based on pier vibration measurements

Wen-Hwa Wu^{*1}, Chien-Chou Chen^{1a}, Wei-Sheng Shi^{1b} and Chun-Ming Huang^{2c}

¹Department of Construction Engineering, National Yunlin University of Science and Technology,
No. 123, University Road, Touliu, Yunlin 640, Taiwan

²Intelligent Electronic Systems Division, National Chip Implementation Center, National Applied Research Laboratories,
7F, No. 26, Prosperity Road 1, Science Park, Hsinchu City 300, Taiwan

(Received October 21, 2016, Revised April 4, 2017, Accepted April 18, 2017)

Abstract. A recent work by the authors has demonstrated the feasibility of scour evaluation for Kao-Ping-Hsi Cable-Stayed Bridge simply based on ambient vibration measurements. To further attain the goal of scour monitoring, a key challenge comes from the interference of several environmental factors that may also significantly alter the pier frequencies without the change of scour depth. Consequently, this study attempts to investigate the variation in certain modal frequencies of this bridge induced by several environmental factors. Four sets of pier vibration measurements were taken either during the season of plum rains, under regular summer days without rain, or in a period of typhoon. These signals are analyzed with the stochastic subspace identification and empirical mode decomposition techniques. The variations of the identified modal frequencies are then compared with those of the corresponding traffic load, air temperature, and water level. Comparison of the analyzed results elucidates that both the traffic load and the environmental temperature are negatively correlated with the bridge frequencies. However, the traffic load is clearly a more dominant factor to alternate the identified bridge deck frequency than the environmental temperature. The pier modes are also influenced by the passing traffic on the bridge deck, even though with a weaker correlation. In addition, the variation of air temperature follows a similar tendency as that of the passing traffic, but its effect on changing the bridge frequencies is obviously not as significant. As for the effect from the alternation of water level, it is observed that the frequency baselines of the pier modes may positively correlate with the water level during the seasons of plum rains and typhoon.

Keywords: scour monitoring; cable-stayed bridge; pier vibration measurements; stochastic subspace identification; empirical mode decomposition; traffic load; air temperature; water level

1. Introduction

To more effectively maintain the safety and serviceability of critical civil structures such as long-span bridges, a lot of efforts have been made to apply the structural health monitoring (SHM) approach for condition assessment or even damage detection. Foundation scour that excavates the bed material around the piers and abutments has been found to be the primary cause of bridge failures or damages in a lot of areas over the world. Taking Taiwan as an example, the single case of devastating Typhoon Morakot in the summer of 2009 led to the collapse or severe damage of more than 110 bridges, mostly due to foundation scour. Accordingly, accurate evaluation of foundation scour plays a particularly important role in bridge health

monitoring. Several approaches based on installing underwater sensors at or close to the substructure were developed to directly measure the scour depth by exploiting various physical quantities (Wang *et al.* 2012, Xiong *et al.* 2012, Fisher *et al.* 2013, Yu *et al.* 2013). Most of these methods, however, require expensive underwater installation. In addition, their capability to sustain severe floods or debris flows may be of great concerns.

Taking advantage of the advances in sensing technologies and the convenience in conducting ambient vibration measurements, recent studies started to investigate the feasibility of applying vibration-based techniques for a more economical approach of detecting bridge scour. With the traffic-induced vibration measurements on an existing bridge in Northern Italy, Foti and Sabia (2012) found that the consequence of a scoured pier can be recognized from the dynamic response of bridge foundation. Lin *et al.* (2012, 2013) developed a scour detection algorithm according to the relationship between the fundamental frequency of superstructure and the embedded depth of bridge pier established with a finite element model. By examining the static and dynamic response of a single pile or pile groups to scour effects, Kong *et al.* (2013, 2016) proposed three possible methods for detecting bridge scour either with the modal frequency change, bending moment profile, or modal

*Corresponding author, Professor
E-mail: wuwh@yuntech.edu.tw

^aProfessor
E-mail: ccchen@yuntech.edu.tw

^bFormer Master Student
E-mail: m10216206@yuntech.edu.tw

^cDivision Director
E-mail: cmhuang@cic.narl.org.tw

strain profile. Prendergast *et al.* (2013) performed the laboratory and field tests for a piled foundation system to show that the natural frequency of the pile decreases with the increasing scour depth. In addition, the viability of detecting the changes in frequency with the bridge dynamic response to a passing vehicle was also verified (Prendergast *et al.* 2016). Elsaid and Seracino (2014) inspected the potential of simply using the dynamic features of the bridge superstructure to detect scour at the bridge piles and discovered that the horizontally-displaced mode shapes are most sensitive to scour. Most recently, Bao and Liu (2017) presented a comprehensive review of existing studies on scour detection using the natural frequency spectrum of a bridge or a bridge component.

Even though the abovementioned works on vibration-based techniques have demonstrated the great potential of this efficient approach, several important issues still need to be further explored for a successful application in actual scour detection. With the consideration of realistic soil effects, loyal modeling of the interactions between structural components, and cautious simulation of boundary support conditions, a recent work by the authors (Chen *et al.* 2014) developed a scour evaluation method for Kao-Ping-Hsi (KPH) Cable-Stayed Bridge located in southern Taiwan using ambient vibration measurements of its superstructure. The predominant modal frequencies of girder and those of the local pier were first identified. The finite element model of this bridge was then calibrated, principally focusing on the determination of best boundary support conditions to fit the identified girder frequencies. Based on such a globally best fitted model, the optimal soil stiffness was subsequently decided by fitting the critical bridge frequencies with a known deposit height at the pylon. With the determined soil stiffness, the scour depth at a pier was estimated by varying the depth of its supporting soil to match the two sensitive frequencies of local pier modes. Finally, the accuracy of this method was validated by the direct measurement of scour depth. The major contribution of such a work is to verify the feasibility of applying the vibration-based techniques for the scour evaluation of a large-scale real bridge. With a good estimation of the current scour depth in this case, the possibility to conduct the subsequent scour monitoring merely by placing sensors on the pier top seems just few steps away.

To attain the goal of scour monitoring simply based on pier vibration measurements, a key challenge comes from the interference of several environmental factors that may also significantly alter the pier frequencies without the change of scour depth. Quite a few studies in recent years have examined the influences of various environmental factors including the temperature, the traffic load, and the wind speed to gain important insights into this complicated topic. Specifically for cable-stayed bridges, it has been indicated (Ni *et al.* 2007, Li *et al.* 2007, Min *et al.* 2009, Sun *et al.* 2013) that only an extremely large wind speed usually occurred during the invasion of typhoon can induce an observable alternation in bridge frequencies. In general, the environmental temperature and the passing traffic are relatively dominant factors to cause the variation in the

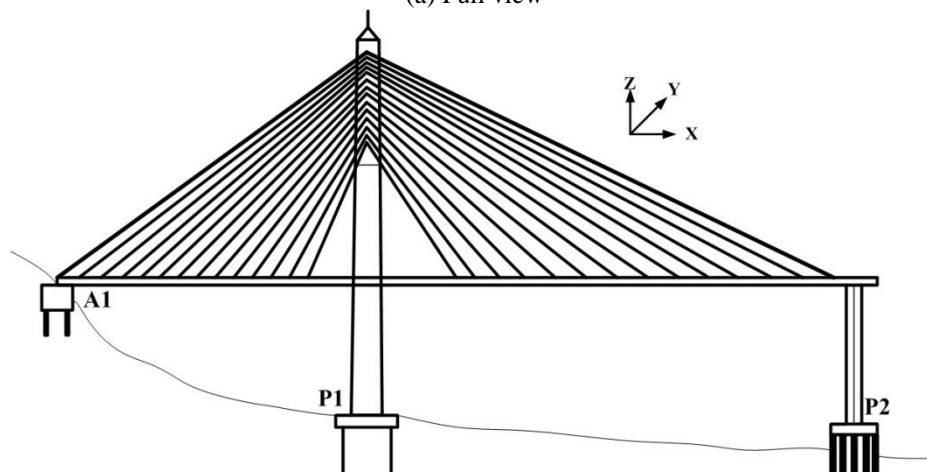
modal frequencies of a cable-stayed bridge (Min *et al.* 2009). Periodic trends of daily and long-term (yearly) variations were clearly observed for the effect of environmental temperature on the bridge frequencies (Li *et al.* 2007, Sun *et al.* 2013), typically associated with an evident time lag possibly resulted from thermal conduction and thermal radiation (Sun *et al.* 2015). As for the passing traffic, its effect on the modal frequencies of a cable-stayed bridge is instantaneous (Li *et al.* 2007, Sun *et al.* 2013). The influence of passing traffic was also found to focus on vertical and torsional modes in lower order (Macdonald and Daniell 2005, Li *et al.* 2007). This effect can produce a reduction over 1% in the bridge frequencies (Zhang *et al.* 2002, Macdonald and Daniell 2005, Li *et al.* 2007) and may increase the corresponding damping ratios (Zhang *et al.* 2002, Chen *et al.* 2010).

Similar attention has been paid to the effects of different environmental factors on the modal frequencies of a suspension bridge to obtain a few tendencies comparable to those for cable-stayed bridges (Cross *et al.* 2010, Westgate 2012, Apaydin *et al.* 2012, Laory *et al.* 2014, Westgate *et al.* 2015). First of all, the variation of wind speed is trivial to the change in the modal frequencies of a suspension bridge (Cross *et al.* 2010). The major roles to alter the bridge frequencies are also played by the environmental temperature and the passing traffic. The increase in either of these two factors would lead to the reduced modal frequencies of a suspension bridge (Westgate 2012, Apaydin *et al.* 2012). More specifically, the lateral modes seem to be more closely effected by the environmental temperature. On the other hand, the passing traffic may have noticeable influences on the modes in all the different directions, especially the vertical and torsional modes (Westgate 2012, Westgate *et al.* 2015). In addition to the three environmental factors mentioned above, recent studies in scour monitoring also started to investigate the effect of water level on the bridge pier (Li 2012, Lin 2013).

As an extension to the previous work (Chen *et al.* 2014) that has successfully evaluate the scour depth of KPH Cable-Stayed Bridge, the current study aims to clarify the variation in the modal frequencies of this bridge induced by several environmental factors such that the subsequent scour monitoring can be more accurately performed. Different sets of pier vibration measurements were taken for a longer duration under various environmental conditions including the season of plum rains, regular summer days without rain, and the typhoon period. These signals are first analyzed with an improved stochastic subspace identification (SSI) algorithm combining the alternative stabilization diagram and the hierarchical sifting process to more conveniently identify reliable modal parameters (Wu *et al.* 2016a, Wu *et al.* 2016b). After obtaining the time variation of each identified modal frequency from the continuous pier measurements of several days, the empirical mode decomposition (EMD) technique is further utilized for systematically extracting the time-varying baselines of different modal frequencies. Finally, the variations of modal parameters identified from each measurement are extensively compared with those of the corresponding traffic load, air temperature, and water level to assess the



(a) Full view



(b) Illustration

Fig. 1 Kao-Ping-Hsi Cable-Stayed Bridge

environmental effects on the vibration-based approach for scour monitoring.

2. Brief review of previous results

To clearly provide the backgrounds for this work, the results in Chen *et al.* (2014) are concisely reviewed in this section.

2.1 Kao-Ping-Hsi Cable-Stayed Bridge

Kao-Ping-Hsi Bridge locates in Freeway No. 3 of Taiwan. It connects Kaohsiung and Pingtung, separated by a major river Kao-Ping-Hsi, and consists of six units with a total length of 2617 m. The first unit at the northern end is an unsymmetrical single-pylon cable-stayed bridge, the third longest of its kind in the world. Kao-Ping-Hsi Cable-Stayed Bridge, illustrated in Fig. 1, comprises two spans and is 510 m in length. The main span made by steel box girders is with a length of 330 m and crosses the main flowing channel of river. The side span, on the other hand, is built by pre-stressed concrete box girders to have a length of 180 m. The reinforced concrete pylon (P1 pylon) in an inverse Y shape is 183.5 m tall and sits on two foundations of diaphragm walls. The main bridge girder is primarily supported by the cable system consisting of 15 pairs of stay

cables on each side of the pylon. Besides, the two ends of bridge girder are supported by a pier (P2 pier) and an abutment (A1 abutment), respectively. P2 pier is next to one of the river banks and stands on a foundation of group piles with a depth of 28 m, while A1 abutment is supported by a foundation of diaphragm walls.

2.2 Ambient vibration measurements and FE modeling

At the end of 2010, ambient vibration measurements for KPH Cable-Stayed Bridge were conducted to broadly cover the bridge decks at both the main and side spans, the interior of the main span steel box girder, and the top of P2 pier. The measurements on the bridge deck include the vertical (gravity), horizontal (river), and axial (driving) direction for obtaining the modal parameters of bridge in all these directions. Moreover, the measurements inside the steel box girder were limited to the vertical direction for identifying the parameters of the torsional modes. As for the measurement on the top of P2 pier, it was taken along the axial direction of bridge in which the pier top is not constrained. The fast Fourier transform (FFT) and an averaged smoothing technique were applied to identify the modal frequencies of KPH Cable-Stayed Bridge based on the Fourier amplitude spectra of measured signals. Eventually, the frequencies for the first three flexural modes

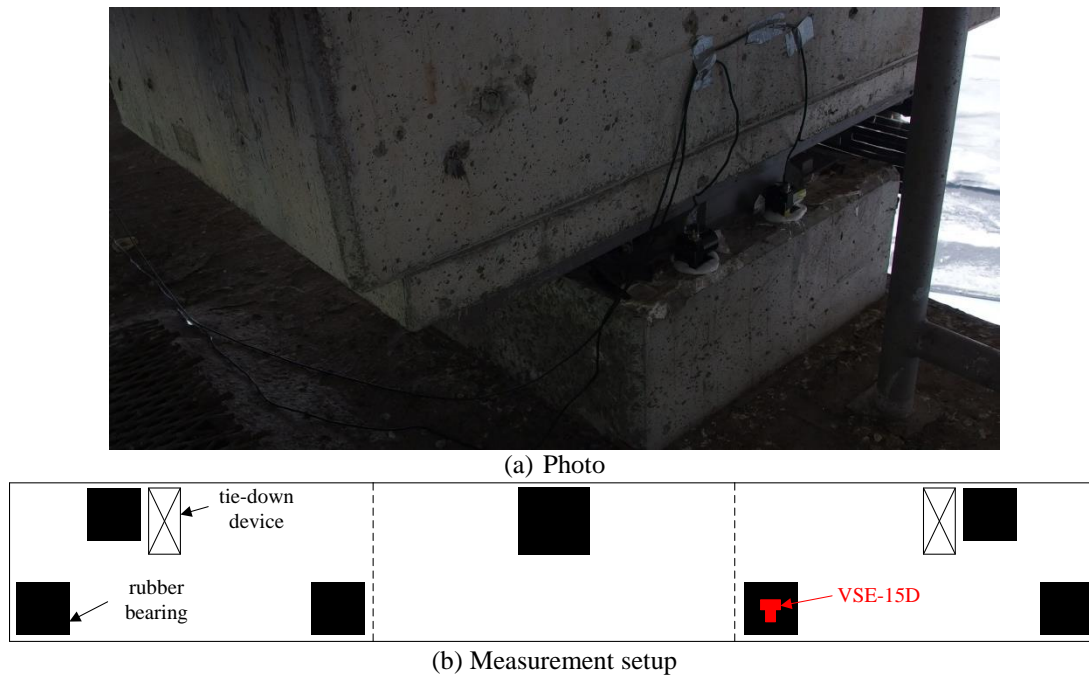


Fig. 2 Measurement at pier P2 of Kao-Ping-Hsi Cable-Stayed Bridge

in vertical direction, the first three flexural modes in horizontal direction, the first two translational modes in axial direction, and the first two torsional modes could be confidently obtained for the bridge deck. In addition, two vertically flexural modes for P2 pier were also identified.

Based on the ten modal frequencies of girder covering different vibration directions, an effective finite element (FE) model of the bridge was then constructed with SAP2000 software to best fit the on-site measurements. It should be noted that the modeling of soil surrounding the foundations was simplified by equivalent springs with the coefficients determined from available drilling reports according to the average of two commonly adopted formulas. With further consideration of actual boundary support conditions to modify the FE model, the errors between the identified and FE modal frequencies were generally kept to be under 2%.

2.3 Evaluation and verification of scour status for pier P2

During the period between late 2010 and early 2011, it was observable that the soil deposit was raised up to 5 m high above the top of foundation at pylon P1. On the contrary, the foundation of pier P2 was under the water level and its scour depth needed to be evaluated. Since the formulas for equivalent soil springs only provide a rough estimation of soil stiffness, it is necessary to further tune the soil stiffness according to the actual structural response measurements for a more accurate scour evaluation. It was fortunate in the case of KPH Cable-Stayed Bridge that the soil level was known at pylon P1. Besides, all the modal frequencies of bridge girder in different directions were found to be unaffected by pier P2 and the soil surrounding

its foundation system through the FE analysis. Taking advantage of these characteristics, the optimal soil stiffness was first determined by fitting the relevant bridge frequencies (the first horizontally flexural mode and the second torsional mode) with a given deposit height at pylon P1.

After the determination of optimal soil stiffness, the frequencies for the first two vertically flexural modes of local pier were discovered to be most sensitive to the change of scour depth and then employed as the basis to evaluate the scour depth at pier P2. It was found that the frequency values of these two modes are approximately decreased by 1% and 4%, respectively, with one meter of increasing scour depth of soil. Several values of scour depth were considered and the average relative error between the identified and FE modal frequencies attained its minimum value in the case of 3.5 m. This indicates that 3.5 m is the most possible scour depth at pier P2 of KPH Cable-Stayed Bridge. To verify the accuracy of this evaluation, a straightforward scheme was designed to directly measure the scour depth of pier P2. Two locations around the foundation of pier P2 were selected to obtain the scour depths of 3.4 m and 4.3 m. Considering that the soil level surrounding pier P2 was not uniform, both of the two measured values are in good agreement with the evaluated value of 3.5 m.

3. Pier vibration measurements

It is clear from the results in Chen *et al.* (2014) that the frequencies for the first two flexural modes of pier P2 moving in the vehicle direction can usually be identified from the vibration measurements on the pier top and are most sensitive to the change of scour depth. Therefore, the

ambient vibration measurements for scour monitoring can be focused on pier P2. Different measurement locations on the pier top basically do not affect the identification of the two interested pier frequencies and the measurement setup of this study is shown in Fig. 2.

The broad-band servo velocity-meter VSE-15D from Tokyo Sokushin was employed to measure the velocity signal along the axial direction and the sampling rate was set at 200 Hz. In the current paper, four sets of pier vibration measurements taken in May, July, August, and September of 2015 are examined and analyzed to investigate the environmental effects on the pier frequencies in scour monitoring.

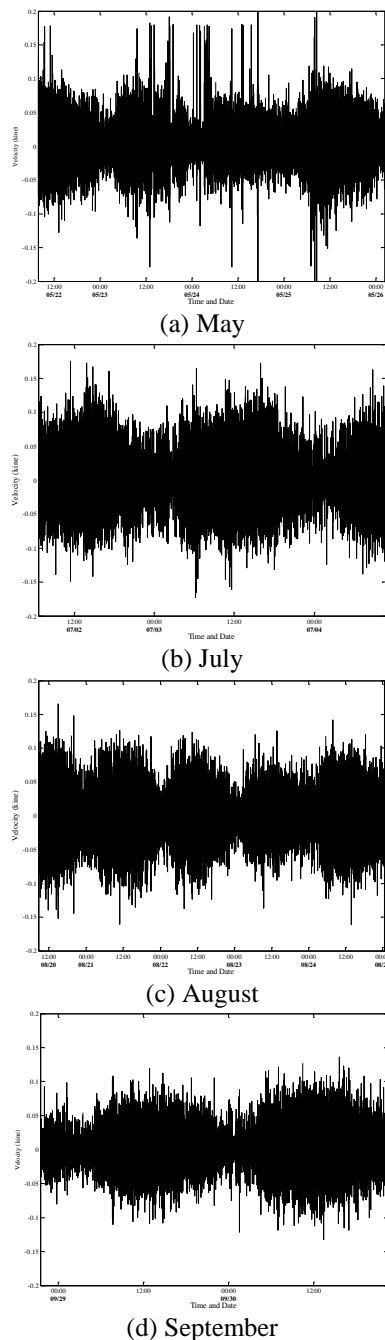


Fig. 3 Four sets of pier vibration measurements conducted in 2015

The first measurement from May 22 to May 26 to

collected 90 hours of pier vibration signal was conducted during the season of plum rains in Taiwan. It was expected that the heavy rains in these few days may induce light scour with an observable decrease in pier frequencies. The results of analysis discussed in the subsequent sections will show that the trend obtained is quite the opposite to indicate the possible influence of water level. To obtain more data for further comparisons, the second measurement from July 2 to July 4 and the third measurement from August 20 to August 25 were conducted to collect 52 hours and 113 hours of pier vibration signal, respectively, under normal summer days without raining. As for the fourth measurement with a length of 48 hours between September 28 and September 30, it was collected from few hours before Typhoon Dujuan quickly moved to reach Taiwan until the time when KPH roughly recovered its pre-typhoon water level. The measured velocity histories in the unit of kine (cm/sec) for these four cases are plotted in Fig. 3. It can be evidently observed from Fig. 3 that the pier response mostly induced by the traffic passing through the bridge deck is generally larger during the day time and usually reaches its minimum at midnight. Furthermore, the measurement in May apparently contains more abrupt peaks than the other three sets of measurement. This phenomenon is due to the fact that the wire connecting the velocity-meter to the data acquisition unit was not deliberately fastened in the first measurement of May. Such a problem was ameliorated in the latter three measurements to eliminate the inaccurate vibration signal induced by possible wire movements under strong winds.

4. Analysis based on improved stochastic subspace identification

Instead of applying FFT to identify the modal frequencies from pier vibration measurements as in Chen *et al.* (2014), an improved SSI algorithm recently developed by the authors (Wu *et al.* 2016a, Wu *et al.* 2016b) is adopted in this study to obtain more reliable frequency values. This technique is briefly described in the first subsection, followed by discussing the identified modal parameters from the pier measurements in the second subsection.

4.1 Alternative stabilization diagram and hierarchical shifting process

The procedures of the covariance-driven SSI start from systematically constructing a Hankel matrix from the measured output vectors with the selection of a time lag parameter i . Multiplication of the two equally divided submatrices from the Hankel matrix leads to the approximation of the so-called Toeplitz matrix. Singular value decomposition can then be conducted on this matrix to obtain the discretized system matrix in the state space with a chosen system order parameter n . Accordingly, it is obvious that the time lag parameter and the system order parameter have to be prescribed in performing the SSI analysis. Theoretically, the time lag parameter specifies the construction of a Hankel matrix from the measured signals

and the subsequent modal parameters identified in the SSI analysis should be insensitive to its value if the excitation is close to the white-noise assumption. It is certainly not so, however, when the excitation is narrowly banded. As for the system order parameter, a value of n sufficiently larger than the number of physical modes within the interested frequency range is usually chosen to assure the incorporation of more contributing modes. The use of high model orders may also result in the inclusion of spurious numerical modes, but is necessary for identifying weakly excited modes and can be helpful to model the noise always existed in measured data.

The determination of modal parameters with the SSI analysis conventionally requires constructing the stabilization diagram to observe the stability of the identified results with the increasing value of n under a designated value of i . Nevertheless, the performance of stabilization diagrams for the applications in civil structures can be significantly affected by the selection of time lag parameter. An effort was made in Wu *et al.* (2016b) to explain this discrepancy in identifying the modal parameters of a stay cable. A critical threshold for the time lag parameter to produce stable identification results was further established. Inspired by this criterion, Wu *et al.* (2016b) further proposed an alternative stabilization diagram which exhibits the gradually increased time lag parameter i along the ordinate and the corresponding modal frequencies along the abscissa under an assigned value of the system order n . By first examining the Fourier amplitude spectra of cable signals, it was suggested to choose the system parameter n that is safely greater than twice of the observable peaks and determine the fundamental period of cable for setting the lower limit to the critical threshold. In addition, the upper limit of time lag parameter is decided by the need in the subsequent processes to extract reliable modal parameters. A hierarchical sifting process including three stages was further developed in Wu *et al.* (2016a, b) to systematically and automatically extract reliable modal parameters from the alternative stabilization diagram. This improved SSI algorithm will be demonstrated in the analysis of the next subsection for identifying the modal parameters of bridge from the pier measurements.

4.2 Identified modal parameters

Each of the four measurements illustrated in Fig. 3 is divided into non-overlapping segments with a duration of 1 hour. In other words, the measurements in May, July, August, and September can be split into 90, 52, 113 and 48 segments, respectively. A typical segment of 1 hour is depicted in Fig. 4(a) and its corresponding Fourier amplitude spectrum is displayed in Fig. 4(b). It has been reported in Chen *et al.* (2014) that the frequencies for the first two vertically flexural modes of pier P2 are approximately with the values of 1.1 Hz and 4.2 Hz, respectively. To more stably identify these two frequencies for each segment of 1 hour, the mode separation technique is applied to extract one interval from 0.9 Hz to 1.2 Hz and the other from 4.1 Hz to 4.4 Hz, as also shown by the

vertical red lines in Fig. 4(b). Inverse Fourier transform is then taken to obtain the time history corresponding to the frequency content in each interval. The improved SSI algorithm reviewed in the previous subsection is eventually applied to process both of the separated time histories and the corresponding alternative stabilizations are plotted in Fig. 5. It should be noted that two stable frequencies can be identified in the range from 0.9 Hz to 1.2 Hz. On the other hand, only one stable frequency exists in the range from 4.1 Hz to 4.4 Hz. Again, compared with the identified frequencies reported in Chen *et al.* (2014), the frequency with a value near 0.98 Hz is associated with a bridge deck mode coupled in the vertically flexural and the vehicle directions and will be denoted by BV-A. In addition, the other two stable frequency values corresponding to the first two flexural modes of pier P2 in the vehicle direction will be signified by PIER1 and PIER2, respectively.

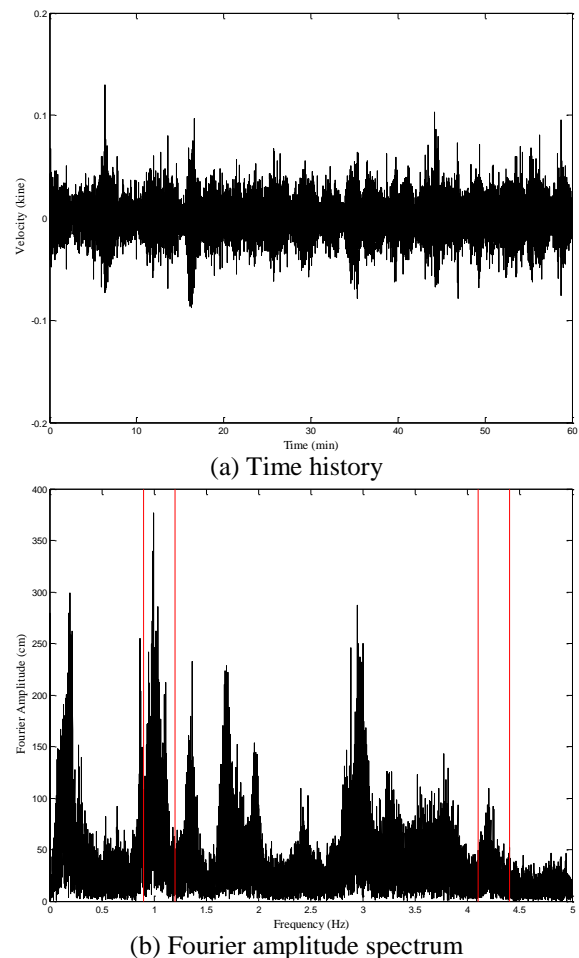


Fig. 4 An example with the extracted record of 1 hr for SSI analysis

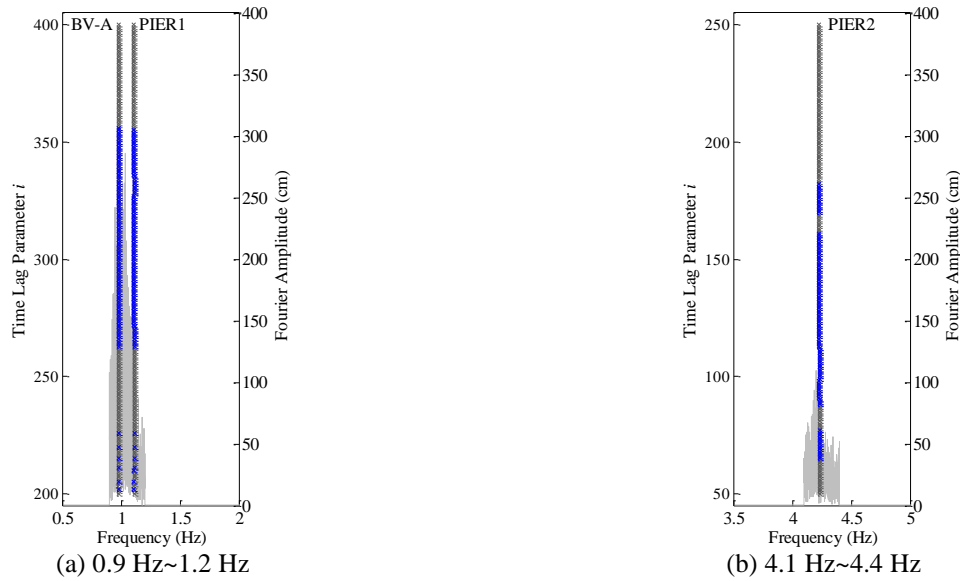


Fig. 5 Alternative stabilization diagrams and results after first shifting stage for the two extracted signals

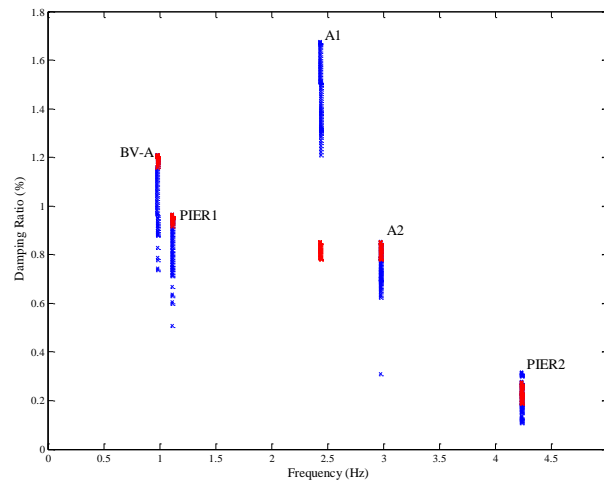


Fig. 6 Results after second shifting stage for the two extracted signals

For each clustered group of frequency values exhibited in Fig. 5, the first stage of sifting process proposed in Wu *et al.* (2016b) is employed to extract 100 closest values symbolized by blue cross signs in Fig. 5. For each group surviving from the first stage, all the damping ratios corresponding to its 100 frequency values are further sifted in the second stage with similar techniques to filter 50 most closed values. Simultaneously presenting the modal frequencies and damping ratios, Fig. 6 portrays the results after the second stage of sifting with red circles to denote the 50 selected frequency and damping values in each group. The mean of these 50 values in each group is then taken as the identified frequency or the damping ratio for the corresponding mode. After performing the SSI analysis to identify the frequencies and damping ratios of modes BV-A, PIER1, and PIER2 for each segment of 1 hour, the variations of all the modal frequencies and all the damping ratios identified from each measurement are displayed in Figs. 7 and 8, respectively. From the small-scale plots

illustrated in Fig. 7, no significant variation can be observed for the modal frequency of BV-A, PIER1, or PIER2. However, there seems to exist periodic fluctuations that will be carefully examined with the variations of different environmental factors in the next section. As for the damping ratios, the trends shown in Fig. 8 indicate relatively stable value for each mode to reflect the reliability and accuracy of the applied SSI algorithm. More specifically, the damping ratios of modes BV-A and PIER1 are both in the neighborhood of 1%, while that of mode PIER2 is with an apparently lower value at around 0.3%.

Emphasis needs to be further made on the validity of identifying the bridge deck modes from the pier measurements. It has been previously discovered and verified by the authors (Chen *et al.* 2008, Wu *et al.* 2016b) that certain modal frequencies and damping ratios of bridge deck can be accurately identified from the cable vibration measurements. Thus, it is not unexpected that the modal parameters of bridge deck can be similarly unveiled from the pier measurements.

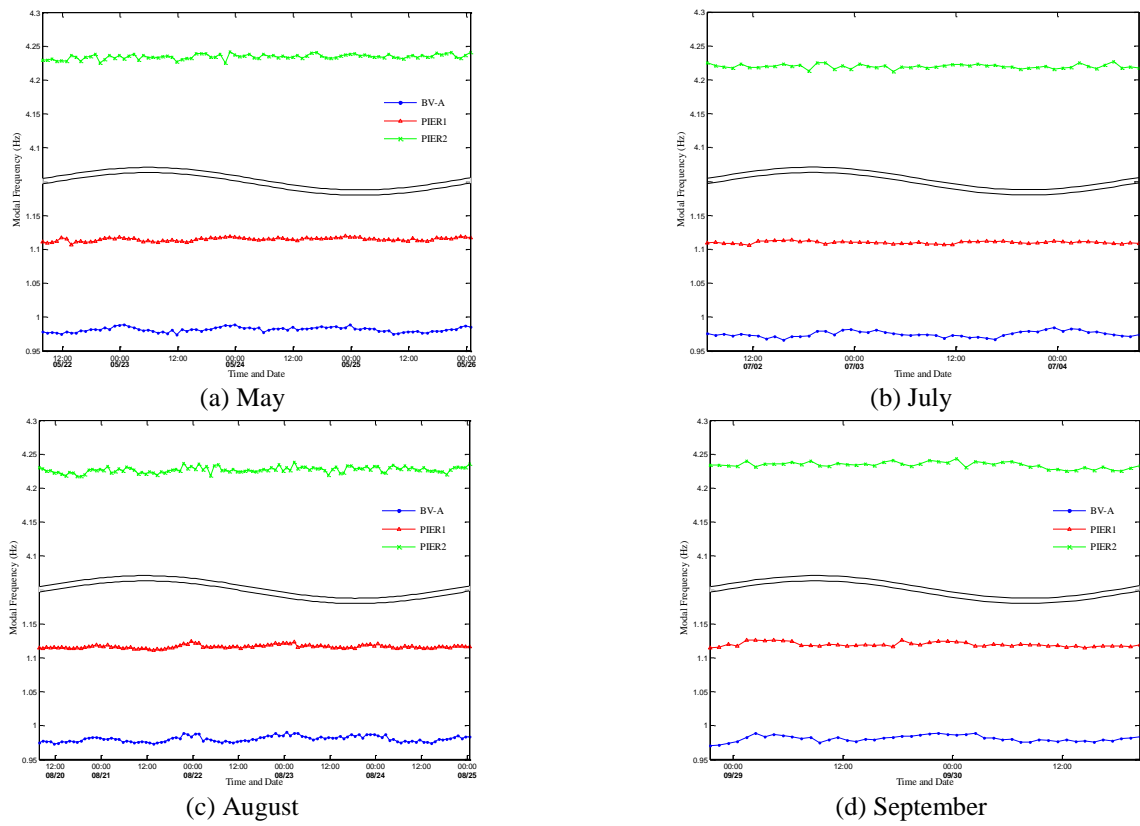


Fig. 7 Identified modal frequencies for four sets of pier vibration measurements conducted in 2015

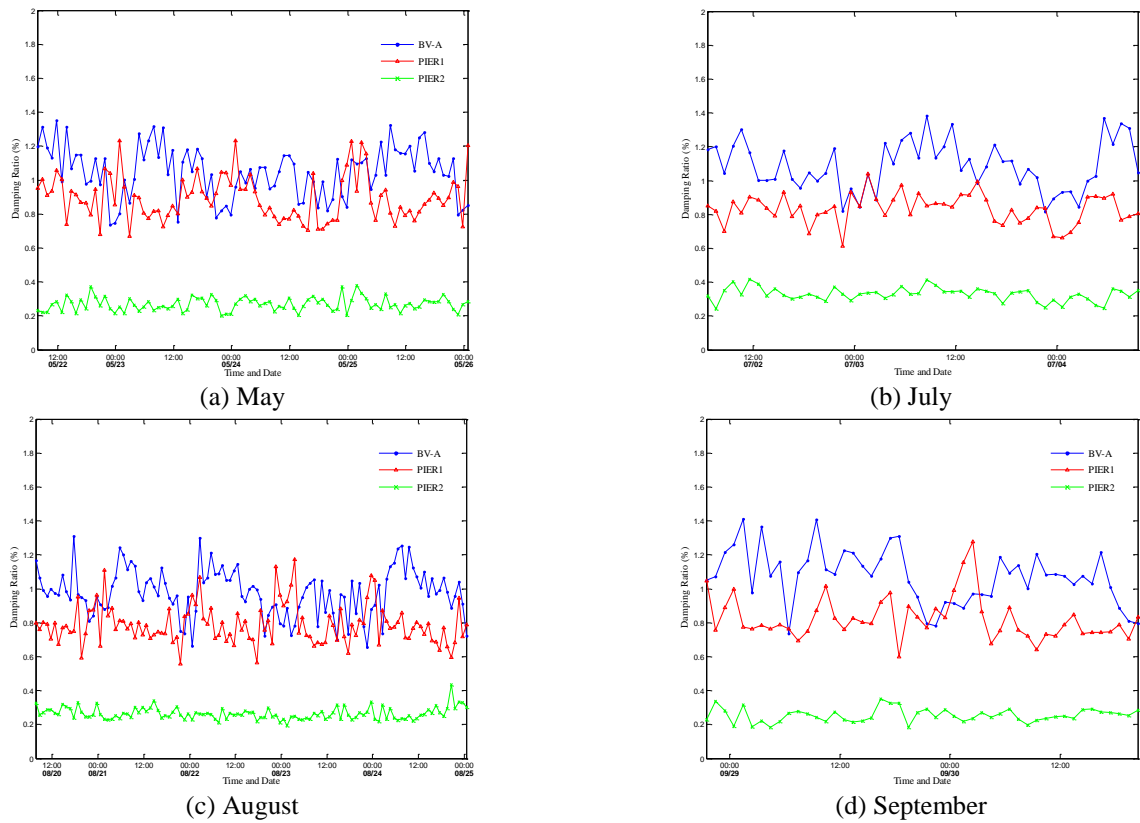


Fig. 8 Identified damping ratios for four sets of pier vibration measurements conducted in 2015

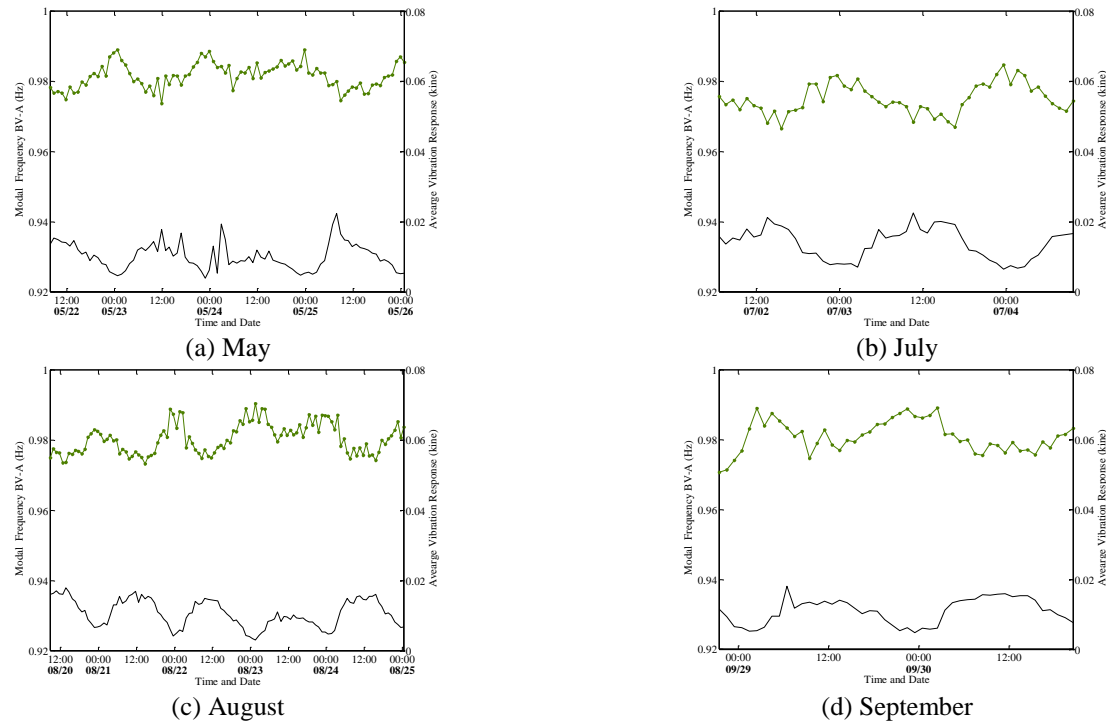


Fig. 9 Comparison between the modal frequency of BV-A and the average vibration response

5. Investigation of environmental effects

To lucidly inspect the variation tendencies for the modal frequencies of BV-A, PIER1, and PIER2, the large-scale plots for these results are extensively examined in this section together with those of the corresponding traffic load, air temperature, and water level.

5.1 Passing traffic represented by average vibration response or ETC record

It should be noted that the vibration response in the vehicle direction obtained from the measurement on the pier top may faithfully reflect the instantaneous effect of the traffic passing through the bridge deck. Consequently, without the need of any further effort in measurements, the standard variation for each hour of the measured velocity history is conveniently calculated to obtain the time histories of average vibration response for representing the variation of passing traffic in this study. Besides, the detailed records of the classified passing vehicles between any two interchanges of a freeway in Taiwan can be directly accessed through the website of Far Eastern Electronic Toll Collection (FETC) Co, Ltd since the launch of the electronic toll collection (ETC) system at the beginning of 2014. These records can also serve as a good reference for the passing traffic.

The variation for the frequency of mode BV-A from each measurement is portrayed in Fig. 9 with a green line. Moreover, the variation of the average vibration response is also presented by a black line in the same figure. Similarly, Figs. 10 and 11 plot the corresponding results for modes

PIER1 and PIER2. Fig. 9 clearly reveals that the bridge deck frequency BV-A is strongly correlated to the average vibration response of P2 pier representing the passing traffic. More specifically, the heavy passing traffic in the day time would increase the effective mass of the bridge deck and consequently decrease its modal frequencies. On the other hand, the light passing traffic around midnight obviously has the reverse effect. The correlation coefficient between the frequency of mode BV-A and the average vibration response can go as high as -0.898 for the measurements in July and -0.902 for the measurements in August. The corresponding correlation coefficient, however, is with a pretty low value of -0.324 for the measurements in May containing a few inaccurate peak responses caused by wire movements under strong winds. As for the case in September under Typhoon Dujuan, the associated correlation coefficient is with a moderate value of -0.567 . Further examination of Figs. 10 and 11 discloses that the pier modes PIER1 and PIER2 are also affected by the passing traffic on the bridge deck, but with a milder correspondence. In addition, this effect is more dominant on PIER1 than PIER2. The range of frequency variation for mode PIER1 in all the four sets of measurements is around 1%, while that for mode PIER2 is about 0.8%.

After adopting the average vibration response as an indicator for the passing traffic to compare with the variations of identified bridge frequencies, the corresponding ETC records are further inspected to confirm the validity of this representation. The details of the passing vehicles on a freeway in Taiwan are totally recorded by the ETC system and can be divided into five categories including sedans, pick-up trucks, buses, freight trucks, and coupling trucks.

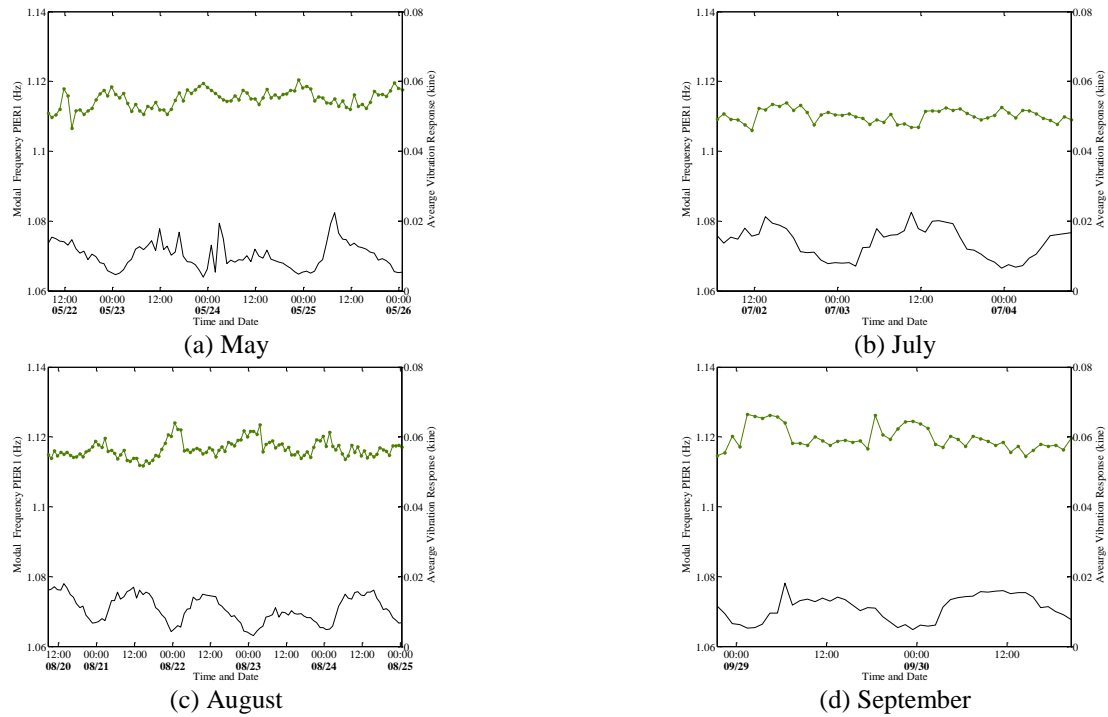


Fig. 10 Comparison between the modal frequency for PIER1 and the average vibration response

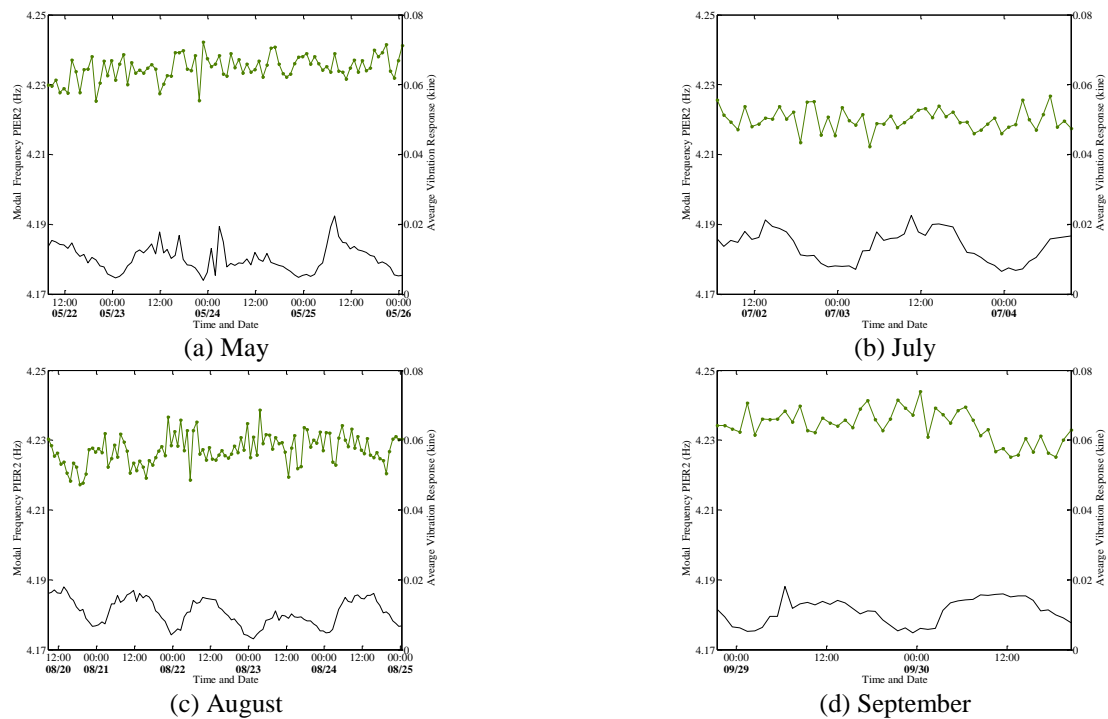


Fig. 11 Comparison between the modal frequency for PIER2 and the average vibration response

For accurately corresponding to the live loads resulted from the passing traffic, the reported weights for various common models of vehicles in all the five categories are investigated together with the consideration of normally carrying weights to determine their approximate weight ratios as

1 : 2 : 14 : 15 : 29. According to the classified ETC records for the passing vehicles between the two interchanges enclosing KPH Cable-Stayed Bridge, the number of sedans running on this segment of freeway is generally much larger than those of the other four categories. Therefore, the passing number per hour for sedans and that for the weighted total traffic in a unit of

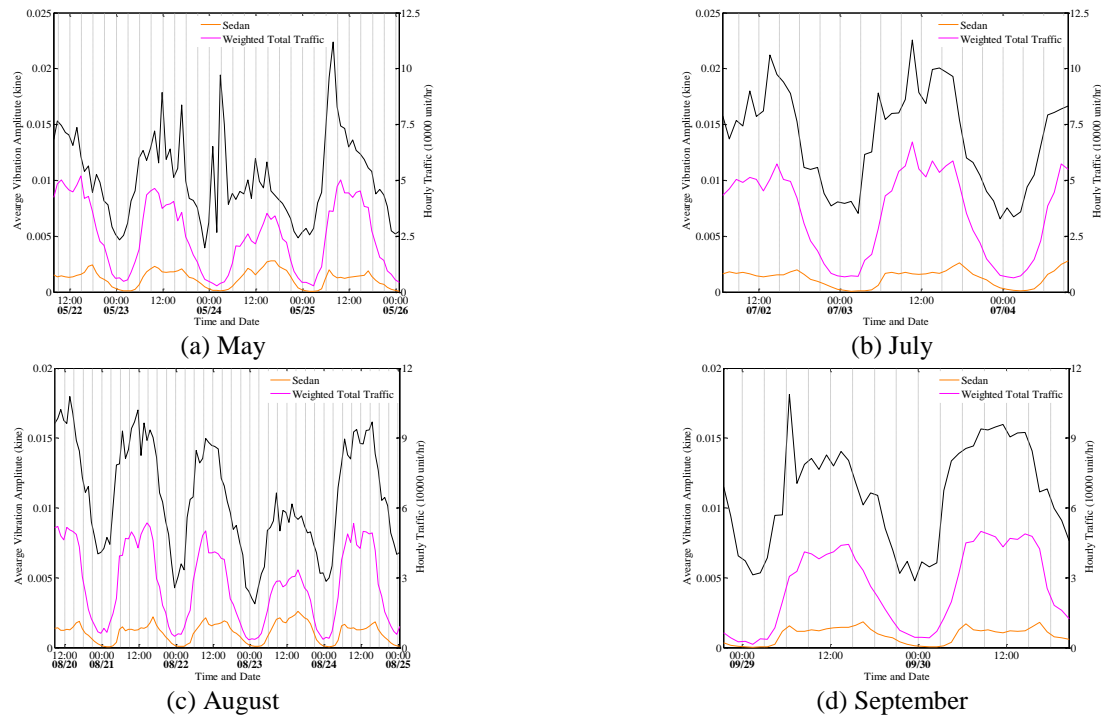


Fig. 12 Comparison between the average vibration response and the ETC records

sedan are plotted with an orange line and a purple line, respectively, in Fig. 12 to compare with the average vibration response depicted with a black line.

As expected, observation of the three curves with different colors in each plot of Fig. 12 evidently indicates that the average vibration response is closely correlated with the weighted total traffic rather than the number of passing sedans (or approximately the number of total passing vehicles). Taking the two Sundays of May 24 illustrated in Fig. 12(a) and August 23 illustrated in Fig. 12(c) as good examples, the number of passing sedans is larger than the other days because of holidays. The weighted total traffic, however, is apparently reduced in these two days due to the significant decrease in freight trucks and coupling trucks with heavy weights. As for the average vibration response, it obviously follows the trend of the weighted total traffic to demonstrate a clear reduction on Sundays. Careful examination of several irregular peaks exhibited in Fig. 12(a) for the variation of the average vibration response between 12:00 of May 23 and 12:00 of May 25 further unveils that the average vibration response is more faithfully related to the bridge deck frequency BV-A than the weighted total traffic. These irregular peaks are not observed in the corresponding variation of the weighted total traffic, but clearly reflected in that of the bridge deck frequency BV-A as shown in Fig. 9(a).

5.2 Air temperature

The air temperature record from a weather station of Central Weather Bureau (CWB) 4.5 km downstream from KPH Cable-Stayed Bridge is adopted in this study to probe the temperature effect. The variation of air temperature for each

measurement is plotted by a yellow line in Fig. 13 to compare with that for the frequency of mode BV-A depicted with a green line. The corresponding results for mode PIER1 are similarly presented in Fig. 14, while the same comparison for mode PIER2 is not included in this paper because no recognizable correlation can be found in that case. Figs. 13 and 14 suggest that the environmental temperature may also play a certain role in alternating the frequencies of bridge deck or pier with a similar but slighter effect compared to the passing traffic. Nevertheless, the variation of air temperature typically follows a similar tendency of the passing traffic to be increased during the daytime and decreased in the nighttime. It is consequently difficult to distinguish the effects of these two environmental factors unless more delicate comparisons can be made. If the attention is focused on the two cases in July and August with a larger variation in temperature during the measurement, it would be easy to discover that the peak values for the frequencies of modes BV-A and PIER1 are consistently reached several hours before the air temperature gets to its minima. On the other hand, the peak frequency values of these two modes synchronize much better with the minimum values of the average vibration response in all the different measurements as shown in Figs. 9 and 10. Therefore, it is true at least for KPH Cable-Stayed Bridge that the environmental temperature effect on the bridge deck or pier frequency is certainly not as important as that of the passing traffic. To be more precise, the variation range of frequency for mode BV-A is around 1.5% during the May measurement with a temperature variation of 3°C as shown in Fig. 13(a). In contrast, the variation range of frequency for mode BV-A goes beyond 2% during the July and September measurements with a temperature variation of 10°C as shown in Figs. 13(b) and 13(d). It is also interesting to note from Fig. 13(c) that the

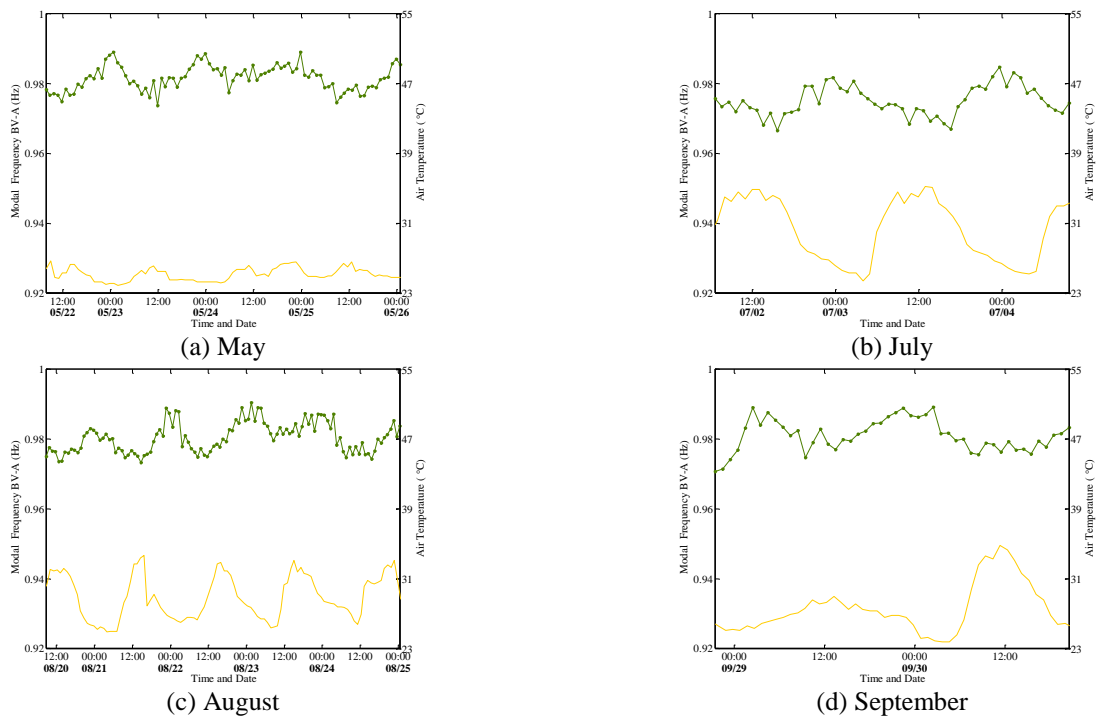


Fig. 13 Comparison between the modal frequency for BV-A and the air temperature

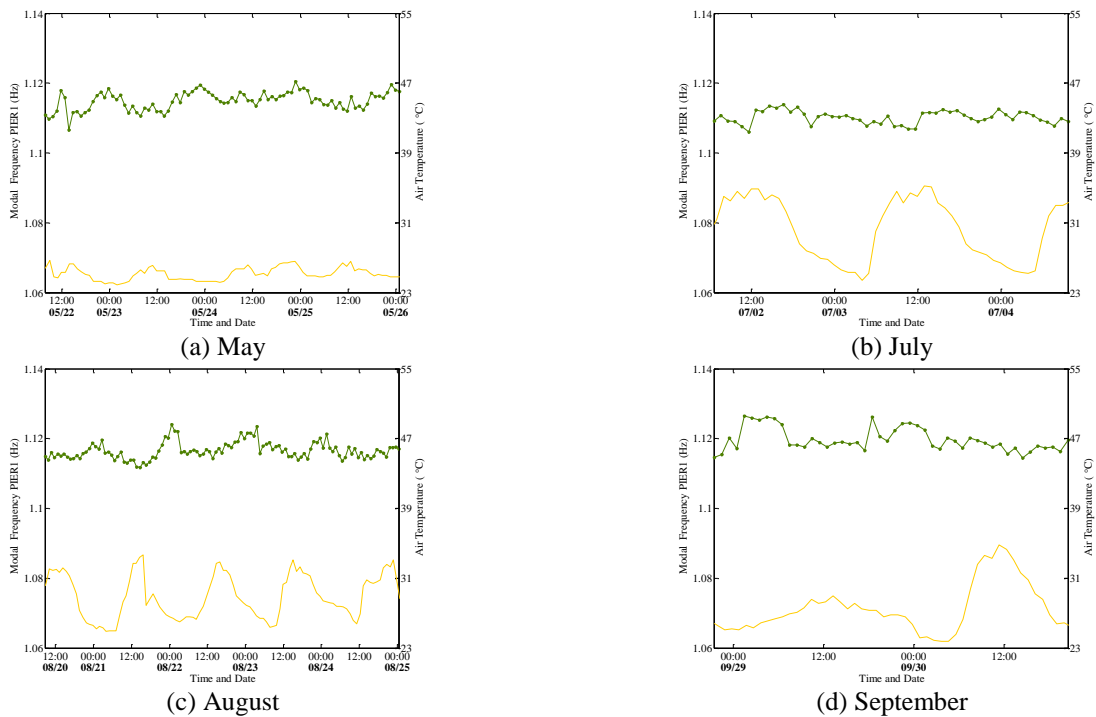


Fig. 14 Comparison between the modal frequency for PIER1 and the air temperature

variations of BV-A frequency and air temperature both fall between the corresponding values of the previous two cases. The above observations naturally lead to the deduction that 10°C variation of the environmental temperature can cause about 0.5% change in the frequency of mode BV-A and the alternating traffic in one day may induce approximately 1.5% change in the same frequency.

This percentage of variation resulted from the traffic load is consistent with the ones reported in the literature (Zhang *et al.* 2002, Macdonald and Daniell 2005, Li *et al.* 2007).

5.3 Water level

The variation of either the passing traffic or air temperature

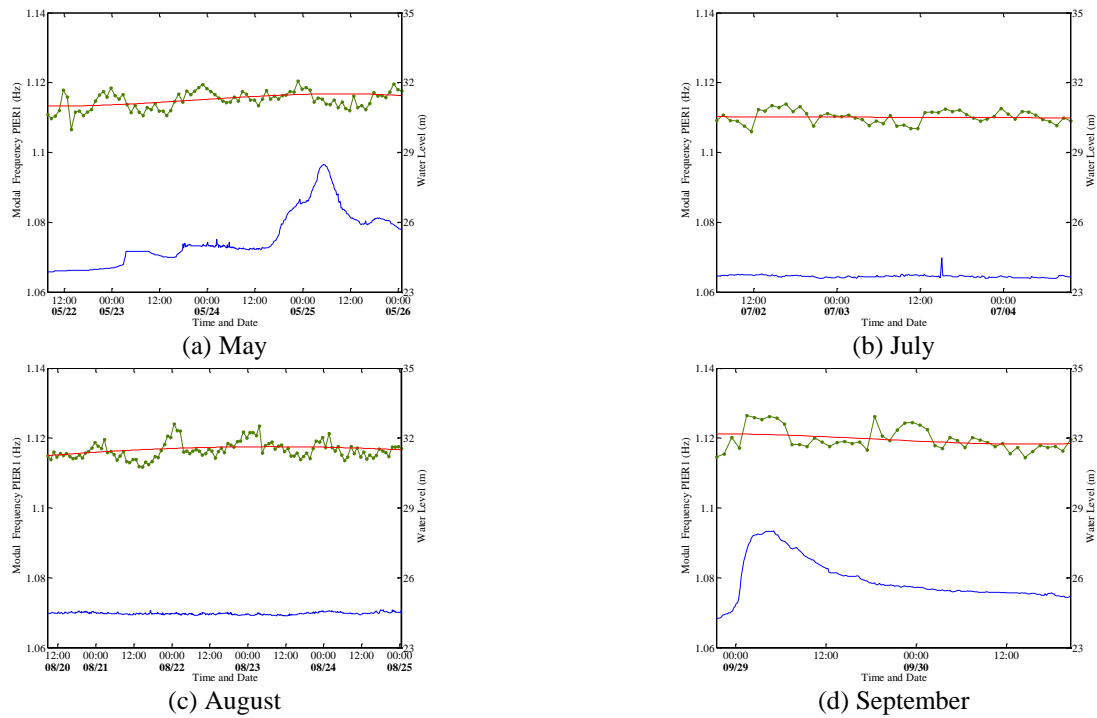


Fig. 15 Comparison between the modal frequency for PIER1 and the water level

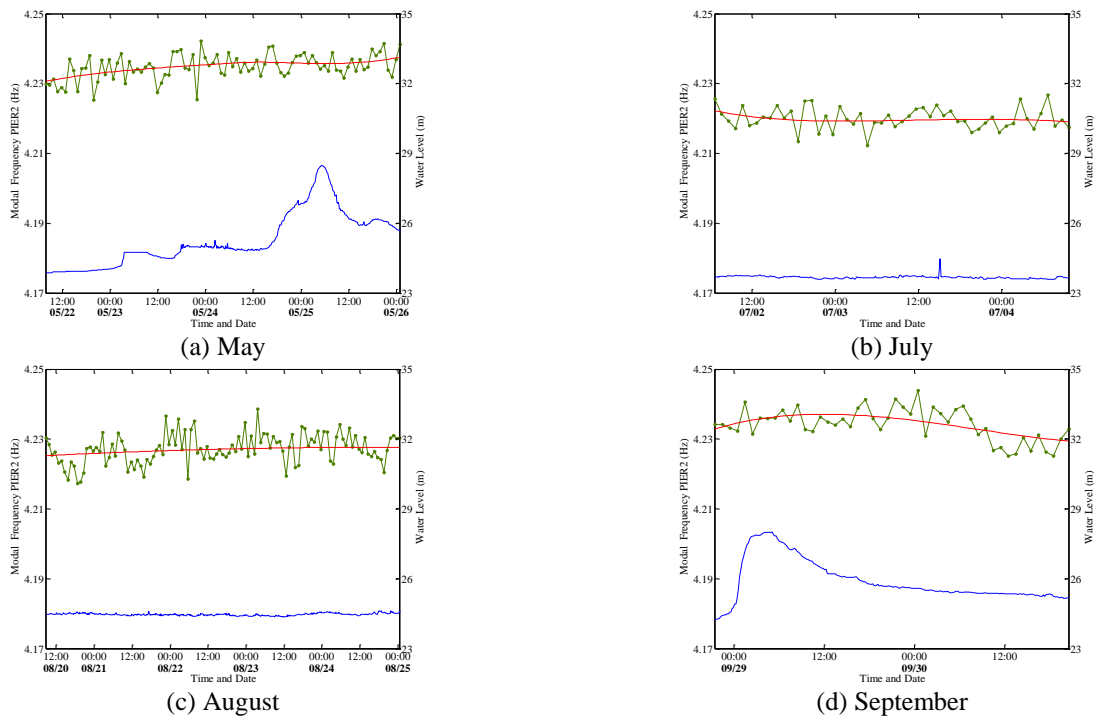


Fig. 16 Comparison between the modal frequency for PIER2 and the water level

is usually in an oscillatory way and goes more rapidly with time. Accordingly, it is feasible to investigate the correlation between these two environmental factors and the bridge frequencies by directly comparing the time histories of their variations. The change in the water level of a river, on the other hand, is relatively irregular and in a much slower pace. Due to this characteristic, the assessment of the minor water level

effect on the bridge frequencies becomes possible if the baselines of their variations are examined. The EMD method is utilized in this study for extracting the baselines in the following discussions and will be briefly described in the next paragraph.

EMD is an adaptive method to decompose a signal into several intrinsic mode functions (IMF) in balanced oscillations

with respect to their zero means (Huang *et al.* 1998). The procedures of EMD usually start with constructing the upper and lower envelopes of the original signal by performing cubic spline interpolations to fit the local maxima and minima, respectively. The average of both envelopes can then be taken to determine a temporary baseline, which is subtracted from the original signal to complete the first round of sifting process. By repeatedly conducting such a sifting process until the number of zero crossings is very close to that of extrema, an IMF can eventually be obtained. Subsequently, subtraction of the extracted IMF from the original signal is carried out to yield the remained signal ready for decomposing the next IMF by similar sifting procedures. This process is reiterated until a monotonic signal, usually referred as the residue, is remained. Overall, the empirical mode decomposition of a signal can be mathematically expressed as

$$h(t) = \sum_{k=1}^m c_k(t) + r(t) \quad (1)$$

where $h(t)$ is the original signal, $c_k(t)$ is the k -th IMF, $r(t)$ is the residue, and m signifies the total number of obtained IMF's. It should be emphasized that the IMF's coming from the EMD process earlier usually have the content in a higher frequency range. Furthermore, the problem of distorted boundaries may appear in the sifting process because no clear control points (extrema) can be exerted at the boundaries in constructing the envelopes with cubic splines. Even though certain efforts have been made to deal with this difficulty (Wu and Huang 2009), special attention still need to be paid in interpreting the boundaries of IMF's or residue obtained from the EMD method. In the analysis of this subsection, the EMD method is adopted to obtain the baselines for the variations of modal frequencies with the residue remained in each process.

The water level record from a hydrographic station of Water Resources Agency (WRA) 500 m upstream from KPH Cable-Stayed Bridge is employed in this study to explore the effect of water level. The variation of water level for each measurement is illustrated with a blue line in Fig. 15 to compare with that for the frequency of mode PIER1 represented by a green line. The EMD method described in the previous paragraph is further utilized to analyze the variation of the pier frequency for determining its baseline displayed with a red line in the same figure. Fig. 16 demonstrates similar results for mode PIER2. The same comparison for mode BV-A is not conducted because such a bridge deck mode is not expected to be influenced by the water level. Figs. 15 and 16 provide enlightening clues to trace the effect of water level on the pier frequencies. Except for the portions close to the boundaries, the baselines in Figs. 15(a), 15(d), 16(a), and 16(d) are very likely to change with the alternating water level during the seasons of plum rains and typhoon. More specifically, the 5 m change of water level for the case in either May or September induces an observable difference in the frequencies of modes PIER1 and PIER2. It can also be noticed that the frequency baseline of mode PIER2 seems to have a stronger correlation with the water level. In contrast, the baselines in Figs. 15(b), 15(c), 16(b), and 16(c) are relatively flat because the water level is basically

unchanged during summer days. The above observations lead to a possible deduction that the pier frequencies would increase with the increasing water level under heavy rainfalls before serious scour actually occurs to reduce the height of soil surrounding the foundation and the pier frequencies.

6. Conclusions

With a recent work by the authors to demonstrate the feasibility of scour evaluation for Kao-Ping-Hsi Cable-Stayed Bridge simply based on ambient vibration measurements, the current study attempts to further investigate the variation in certain modal frequencies of this bridge induced by several environmental factors. Four sets of pier vibration measurements were taken either during the season of plum rains, under regular summer days without rain, or in a period of typhoon. These signals are analyzed with the stochastic subspace identification and empirical mode decomposition techniques. The variations of the identified modal frequencies are then compared with those of the corresponding traffic load, air temperature, and water level to assess the environmental effects.

Comparison of the analyzed results elucidates a few important trends for these environmental effects. First, it is found that both the traffic load and the environmental temperature are negatively correlated with the bridge frequencies. However, the traffic load is clearly a more dominant factor to alternate the identified bridge deck frequency than the environmental temperature. Considering that this bridge locates in a freeway and its main span is made by steel box girders, it is not surprising that the high passing traffic would cause substantial bridge vibrations and become the most crucial environmental factor. It can be further noted that the pier modes are also influenced by the passing traffic on the bridge deck, even though with a weaker correlation. In addition, the variation of environmental temperature follows a similar tendency as that of the passing traffic, but its effect on changing the frequencies of bridge deck or pier is obviously not as significant. Regarding the effect from the alternation of water level typically associated with the occurrence of bridge scour, it is observed that the frequency baselines of the pier modes may positively correlate with the water level during the seasons of plum rains and typhoon.

The clarification of the above environmental effects helps to remove their interference in the variation of identified pier frequencies and is expected to improve the accuracy of scour monitoring with the vibration-based approach. Although no scour was involved in the four sets of vibration measurements analyzed in this study, the effects of environmental factors can still be related with the particular effect of scour presented in the previous work by the authors (Chen *et al.* 2014). As observed from all these measurements in different seasons, the ranges of frequency variation for the two pier modes induced by environmental factors are at the order of 1%. This value is certainly comparable to the corresponding effect resulted from one meter change in scour depth of soil (1% for mode PIER1

and 4% for mode PIER 4). With more comprehensive measurements conducted in the future, it is hoped to investigate the complete scouring process and explore how the effect of scour can eventually be separated from those of involved environmental factors in the next phase of this study.

Other than the conclusions summarized above for assessing the environmental effects, another valuable contribution from this work is to discover that the average vibration response is more closely related to the bridge deck frequency than the weighted total traffic obtained from the ETC records. Such a phenomenon indicates that the standard variation of a vibration measurement can be adopted for effectively representing the live load in structural health monitoring to save a lot of efforts. It should be further emphasized that the above conclusions can be obtained only because an improved SSI method is available to accurately identify the variation smaller than 1% in the modal parameters. In fact, the identified variations of modal parameters to truthfully reflect the effects of various environmental factors also verify the reliability and accuracy of the applied SSI algorithm in return.

Acknowledgments

The authors are grateful to the financial support from the Ministry of Science and Technology of Republic of China under Grant MOST104-2221-E-224-031.

References

- Apaydin, N.M., Kaya, Y., Safak, E. and Alcik, H. (2012), "Vibration characteristics of a suspension bridge under traffic and no traffic conditions", *Earthq. Eng. Struct. D.*, **41**(12), 1717-1723.
- Bao, T. and Liu, Z. (2017), "Vibration-based bridge scour detection: a review", *Struct. Control Health Monit.*, doi: 10.1002/stc.1937.
- Chen, C.C., Wu, W.H. and Liao, J.A. (2008), "Modal frequency identification for cable and girder using ambient cable vibration signals", *J. Chin. Inst. Civ. Hydraul. Eng.*, **20**(4), 509-521.
- Chen, C.C., Wu, W.H., Liu, C.Y. and Lai, G. (2016), "Damage detection of a cable-stayed bridge based on the variation of stay cable forces eliminating environmental temperature effects", *Smart Struct. Syst.*, **17**(6), 859-880.
- Chen, C.C., Wu, W.H., Shih, F. and Wang, S.W. (2014), "Scour evaluation for foundation of a cable-stayed bridge based on ambient vibration measurements of superstructure", *NDT E. Int.*, **66**, 16-27.
- Chen, C.H., Lin, Y.Y. and Yang, S.C. (2010), "Variability of dynamic characteristics of a cable-stayed bridge subject to traffic-induced vibrations", *J. Chung Cheng Inst. Tech.*, **39**(2), 47-56.
- Cross, E., Worden, K., Koo, K.Y. and Brownjohn, J.M.W. (2010), "Modelling environmental effects on the dynamic characteristics of the Tamar suspension bridge", *Proceedings of the 28th IMAC*, Jacksonville, USA, February.
- Elsaid, A. and Seracino, R. (2014) "Rapid assessment of foundation scour using the dynamic features of bridge superstructure", *Constr. Build. Mater.*, **50**(1), 42-49.
- Fisher, M., Atamturktur, S. and Khan, A.A. (2013), "A novel vibration-based monitoring technique for bridge pier and abutment scour", *Struct. Health Monit.*, **12**(2), 114-125.
- Foti, S. and Sabia, D. (2011), "Influence of foundation scour on the dynamic response of an existing bridge", *J. Bridge Eng. - ASCE*, **16**(2), 295-304.
- Huang, N.E., Shen, Z., Long, S.R., Wu, M.C., Zheng, H.H., Yeh, Q., Tung, N.C. and Liu, H.H. (1998), "The empirical mode decomposition and the Hilbert spectrum for nonlinear and non-stationary time series analysis", *P. Roy. Soc. London Ser. A*, **454**, 903-995.
- Kong, X. and Cai, C.S. (2016), "Scour effect on bridge and vehicle responses under bridge-vehicle-wave interaction", *J. Bridge Eng. - ASCE*, **21**(4), 04015083.
- Kong, X., Cai, C.S. and Hou, S. (2013), "Scour effect on a single pile and development of corresponding scour monitoring methods", *Smart Mater. Struct.*, **22**(5), 055011.
- Laory, I., Trinh, T.N., Smith, I.F.C. and Brownjohn, J.M.W. (2014), "Methodologies for predicting natural frequency variation of a suspension bridge", *Eng. Struct.*, **80**, 211-221.
- Li, K.W. (2012), "Assessing the scouring depth and health condition of bridge foundation through the field monitoring and associated structural modeling", M.S. Dissertation, National Taiwan University, Taipei.
- Liao, K.W., Cheng, M.Y., Chiu, Y.F. and Lee, J.H. (2016), "Preliminary bridge health evaluation using the pier vibration frequency", *Constr. Build. Mater.*, **102**, 552-563.
- Lin, F.T. (2013), "Dynamic behavior of bridge foundation under scour - a case study on Shin-Fa Bridge", M.S. Dissertation, National Cheng Kung University, Tainan.
- Lin, T.K., Wang, Y.P., Huang, M.C. and Tsai, C.A. (2012), "Bridge scour evaluation based on ambient vibration", *J. Vibroeng.*, **14**(3), 1113-1121.
- Lin, T.K., Wu, R.T., Chang, K.C. and Yu, S.C. (2013), "Evaluation of bridge instability caused by dynamic scour based on fractal theory", *Smart Mater. Struct.*, **22**(7), 075003.
- Macdonald, J.H.G. and Daniell, W.E. (2005), "Variation of modal parameters of a cable-stayed bridge identified from ambient vibration measurements and FE modelling", *Eng. Struct.*, **27**(13), 1916-1930.
- Min, Z., Sun, L. and Dan, D. (2009), "Effect analysis of environmental factors on structural modal parameters of a cable-stayed bridge", *J. Vib. Shock*, **28**(10), 99-105.
- Ni, Y.Q., Ko, J.M., Hua, X.G. and Zhou, H.F. (2007), "Variability of measured modal frequencies of a cable-stayed bridge under different wind conditions", *Smart Struct. Syst.*, **3**(3), 341-356.
- Prendergast, L.J., Hester, D. and Gavin, K. (2016), "Determining the presence of scour around bridge foundations using vehicle-induced vibrations", *J. Bridge Eng. - ASCE*, **21**(10), 04016065.
- Prendergast, L.J., Hester, D., Gavin, K. and O'Sullivan, J.J. (2013), "An investigation of the changes in the natural frequency of a pile affected by scour", *J. Sound Vib.*, **332**(25), 6685-6702.
- Sun, L., Zhou, Y. and Xie, D. (2013), "Environmental effects on modal frequency of long-span cable-stayed bridges", *J. Chongqing Jiaotong U.*, **32**(6), 1106-1110.
- Sun, L., Zhou, Y. and Xie, D. (2015), "Periodic characteristics of environmental effects on modal frequencies of a cable-stayed bridge", *J. Tongji U.*, **43**(10), 1454-1462.
- Wang, C.Y., Wang, H.L. and Ho, C.C. (2012), "A piezoelectric film type scour monitoring system for bridge pier", *Adv. Struct. Eng.*, **15**(6), 897-905.
- Westgate, R. (2012), "Environmental effects on a suspension bridge's performance", Ph.D. Dissertation, University of Sheffield, Sheffield.
- Westgate, R., Koo, K.Y. and Brownjohn, J.M.W. (2015), "Effect of vehicular loading on suspension bridge dynamic properties", *Struct. Infrastruct. Eng.*, **11**(2), 129-144.

- Wu, W.H., Wang, S.W., Chen, C.C. and Lai, G. (2016a), "Mode identifiability of a cable-stayed bridge under different excitation conditions assessed with an improved algorithm based on stochastic subspace identification", *Smart Struct. Syst.*, **17**(3), 369-389.
- Wu, W.H., Wang, S.W., Chen, C.C. and Lai, G. (2016b), "Application of stochastic subspace identification for stay cables with an alternative stabilization diagram and hierarchical sifting process," *Struct. Control Health Monit.*, **23**(9), 1194-1213.
- Wu, Z. and Huang, N.E. (2009), "Ensemble empirical mode decomposition: a noise assisted data analysis method", *Adv. Adapt. Data Anal.*, **1**(1), 1-41.
- Xiong, W., Cai, C.S. and Kong, X. (2012), "Instrumentation design for bridge scour monitoring using fiber Bragg grating sensors", *Appl. Opt.*, **51**(5), 547-557.
- Yu, X.B., Zhang, B., Tao, J.L. and Yu, X. (2013), "A new time-domain reflectometry bridge scour sensor", *Struct. Health Monit.*, **12**(2), 99-113.
- Zhang, Q.W., Fan, L.C. and Yuan, W.C. (2002), "Traffic-induced variability in dynamic properties of cable-stayed bridge", *Earthq. Eng. Struct. D.*, **31**(11), 2015-2021.